JOURNAL OF CATALYSIS **173,** 501–510 (1998)
ARTICLE NO. CA971951

Characterization and Catalytic Evaluation of SAPO-5 Synthesized in Aqueous and Two-Liquid Phase Medium in Presence of a Cationic Surfactant

M. Montoya-Urbina,* D. Cardoso,* J. Pérez-Pariente,†,[1] E. Sastre,† T. Blasco,‡ and V. Fornés‡

*Federal University of Sao Carlos, Chemical Engineering Department, P.O. Box 676, Sao Carlos 13.565-905, S.P., Brazil; †Instituto de Catálisis y Petroleoquímica, CSIC, Camino de Valdelatas s/n, Campus Universidad Autónoma, 28049 Cantoblanco, Madrid, Spain; and ‡Instituto de Tecnología Química, UPV-CSIC, Avenida de los Naranjos s/n, 46022 Valencia, Spain

Received June 23, 1997; revised October 23, 1997; accepted October 24, 1997

High silica content SAPO-5 was synthesized using aqueous and two-liquid phase systems in presence of hexadecyltrimethylammonium bromide. The scope of the work was to study the effect of the synthesis parameters on the amount of silicon incorporated into the network, the different silicon environments and on the catalytic activity in the *m*-xylene isomerization. The results showed that the use of the two-liquid phase synthesis causes greater incorporation and diversification of the silicon distribution in the SAPO-5 network and therefore, a substantial increase in the material acidity. The maximum catalytic activity in the conversion of meta-xylene was achieved by the samples synthesized via the two-liquid phase method and in the presence of the surfactant with 10 wt% of SiO_2. Silica incorporation above 10% creates greater silicon domains, reducing drastically the catalytic activity of the material.

Key Words: **SAPO-5; synthesis; silicon distribution; *m*-xylene isomerization; cationic surfactant.**

1. INTRODUCTION

Aluminophosphate molecular sieves ($AlPO_4$) represent one of the most novel class of inorganic microporous materials. The discovery of these AlPOs led not only to new structures, but also to new materials, by incorporating several elements other than Al or P (1). The incorporation of silicon into the network structure results in the formation of silicoaluminophosphates, SAPOs, which are able to promote ion exchange and to generate Brönsted acidity. However, the concentration of acid sites is governed by the fraction of total silicon replacing P and P + Al pairs. Indeed, according to the relative weight of both substitution mechanisms, several Si environments are generated, which determine the acid strength of the associated proton (2, 3). Therefore, from the point of view of the potential application of this materials in acid-catalyzed reactions, it would be desirable to have some control on the overall Si substitution mechanism.

In the particular case of the large pore SAPO-5, it has been shown recently (4) that the addition of cationic surfactants to a two-liquid phase gel, in such concentration that a microemulsion is obtained, strongly modifies the Si environment in the crystals. In the case of the very large pore SiVPI-5, samples with enhanced activity in *m*-xylene isomerization are obtained (5).

Within the context of the above mentioned, the scope of our work has been to synthesize SAPO-5 samples from hexanol/water/hexadecyltrimethylammonium gels in a broad range of silicon content and to compare the physicochemical characteristics and the catalytic activity in the reaction of *m*-xylene isomerization of these samples with those obtained from pure aqueous gels. Samples have been also characterized by i.r. spectroscopy after pyridine adsorption/desorption for acidity evaluation and by ^{29}Si MAS NMR in order to determine the nature of the Si environment.

2. EXPERIMENTAL

Synthesis

SAPO-5 was synthesized from gels with the composition

$$Al_2O_3 : P_2O_5 : x_g SiO_2 : a Et_3N : b C_6H_{13}OH : c CTABr : w_g H_2O,$$

where the SiO_2 source was Fumed Silica (Aerosil 200, Degussa) in the case of the aqueous system and tetraethylorthosilicate (TEOS, Merck, 98%) in the case of the two-liquid phase system.

In both systems crystallization was carried out using triethylamine (Aldrich) as template, pseudobohemite (Condea, 74.6% Al_2O_3) and phosphoric acid (Riedel, 85%) as aluminum and phosphorous sources, respectively. In the two-liquid phase system n-hexanol ($b = 4.4$, Fluka)

[1] Author for correspondence. E-mail: jperez@icp.csic.es.

0021-9517/98 $25.00

and hexadecyltrimethylammonium bromide (CTABr, $c =$ 0.072, Panreac, 98 wt%) as surfactant, were added to the reaction mixture. The composition of the reaction mixture was modified in order to obtain different SiO_2/Al_2O_3 ratio (0.2–2.0) in both syntheses. The amount of water used in the synthesis gel was $w_g = 40$ or $w_g = 100$, for the aqueous system and $w_g = 40$ for the two-liquid phase system; a was 1.5 for all samples, except for the one with $w_g = 100$, where $a = 1.0$ was used.

In a typical synthesis procedure for the surfactant containing system ($x_g = 0.2$), 10.24 g of alumina were added on a solution of 16.22 g of phosphoric acid in 45.72 g of water. The mixture is stirred at room temperature for 2 h in a polypropylene bottle. Then, 11.35 g of triethylamine were added and 2 h later a solution prepared from 3.12 g of TEOS and 1.96 g of CTABr in 33.57 g of n-hexanol was added. The stirring was kept for two additional hours, and after this the reaction mixture was introduced in 60-ml stainless steel autoclaves provided with PTFE liners. Two crystallization temperatures were used, 443 and 468 K; the autoclaves were heated in a stove for a crystallization time varied between 30 min and 48 h. The samples used in the acidity measurements and catalytic activity were obtained with a crystallization time of 48 h.

Characterization

Sample crystallinity was estimated from the area of the peaks in the X-ray diffractograms at angles $2\theta \cong 19.7$, 21.0, and 22.3°. The diffractograms were obtained from a PHILIPS PW 1710 diffractometer, using CuKα radiation. The standard sample taken as 100% crystalline for crystallinity evaluation was synthesized using a reaction mixture of composition: $0.2SiO_2 : Al_2O_3 : P_2O_5 : 1.5TEA : 40H_2O$ and crystallized at 443 K for 48 h (sample A1, Table 1).

The silicon content present in the solid was determined by colorimetry using a Shimadzu 2100 UV-visible spectrophotometer. Analysis of the organic material in the silicoaluminophosphates was done in a Perkin Elmer 2400 CHN-analyzer.

In order to eliminate the template, samples were calcined first in nitrogen for 1 h followed by air for 5 h at 823 K, prior to their acid and catalytic evaluation.

Acidity measurements of the SAPO-5 were done through adsorption of pyridine at room temperature onto selfsupported wafers (10 mg $\cdot$ cm^{-2}) after degassing the sample at 673 K overnight. After adsorption, the pyridine was desorbed at three temperatures (423, 523, and 623 K). Then, the infrared spectra in the region of 4000–1300 cm^{-1} were recorded. Measurements were carried out in a Nicolet 710 FTIR Spectrometer.

Solid State ^{29}Si and ^{27}Al MAS NMR spectra were recorded on a Varian VXR-400S WB spectrometer at 79.5 MHz and 104.2 MHz, respectively. The ^{27}Al MAS NMR spectra were recorded with pulses of 0.3 μs (π/18 rad pulse length), a recycle delay of 0.5 s and spinning rates of 7 kHz. For conventional ^{29}Si MAS spectra pulses of 4.2 μs (π/3 rad pulse length) were applied with a 40-s recycle delay and a rotor spinning rate of 5 kHz. The cross polarization (CP) spectra were obtained using a π/2 rad pulse length for proton of 7 μs; the contact time and recycle delay were 3 ms and 5 s, respectively. The ^{29}Si spectra were simulated with standard Varian software. To fit the experimental data a mixture of gaussian and lorentzian (50%) was used for the outermost peaks (−90 ppm and −110 ppm), whereas the other components were fixed to gaussians.

Catalytic Activity

The catalytic activity experiments with *m*-xylene (Scharlau, 99%) were carried out in a differential fixed-bed reactor operating with continuous feed and nitrogen as carrier gas at atmospheric pressure. The reaction temperature was set at 623 K and the reaction conditions, weight of the catalyst or feed flow, were varied in order to obtain conversions of about 5%. The reaction products were analyzed by gas chromatography using a 2 m × 3 mm OD packed column filled with 16% DC-200 methylsilicone oil and 3% Bentone 34 on 80–100 mesh Chromosorb W. A Varian 3700 gas chromatograph provided with a flame ionization detector (F.I.D.) was used in the analysis. Due to coke deposition, initial activities (v_0) at zero reaction time were calculated for each product (6).

3. RESULTS AND DISCUSSION

The solids obtained after crystallization presented only the characteristic diffraction peaks of the AFI structure (7). Table 1 shows the chemical characteristics of some samples used in this work.

The results obtained on silicon incorporation in the SAPO-5, as a function of the silicon content in the synthesis

TABLE 1

Chemical Composition of Some Selected SAPO-5 Samples

Sample[a]	w_g	x_g	Tc (K)[b]	Composition (TO_2 formula)	SiO_2 (wt%)	C (%)[c]
A1	40	0.2	443	$(Si_{0.04}Al_{0.51}P_{0.45})O_2$	3.7	100
A2	100	0.65	443	—	9.3	77
A3	40	1.0	468	$(Si_{0.10}Al_{0.50}P_{0.40})O_2$	9.6	67
A4	40	1.0	443	—	12.7	61
B1	40	0.2	443	$(Si_{0.05}Al_{0.54}P_{0.41})O_2$	4.7	84
B2	40	0.5	443	$(Si_{0.1}Al_{0.48}P_{0.41})O_2$	9.9	73
B3	40	0.5	468	$(Si_{0.13}Al_{0.45}P_{0.42})O_2$	12.7	86
B4	40	2.0	443	$(Si_{0.47}Al_{0.32}P_{0.21})O_2$	46.3	61

[a] A = Synthesis in aqueous system, B = synthesis in two-phases system.
[b] Crystallization temperature. Crystallization time of 48 h.
[c] Crystallinity of "as synthesized" samples.

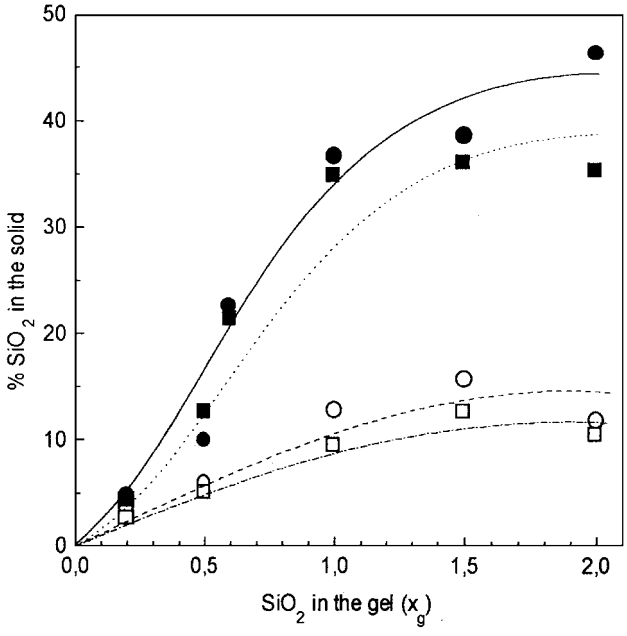

FIG. 1. Incorporation of Si in SAPO-5 as a function of silicon content in the reaction mixture and crystallization temperature. $w_g = 40$; open symbols: Aqueous synthesis, solid symbols: Two-liquid phase synthesis; (○, ●): 443 K, (□, ■): 468 K.

gel and the crystallization temperature, are presented in Fig. 1 for both synthesis methods (aqueous and two-liquid phase). In this figure one can note that up to $x_g = 1.0$ there is a progressive increase in the silicon content in the SAPO-5 with silicon increase in the reaction mixture and this incorporation was slightly higher for the lower synthesis temperature.

Comparison of the two synthesis methods shows that above $x_g = 1$ the SAPO-5 synthesized in the two-liquid phase medium in presence of CTA surfactant incorporates four times more silicon than that in the aqueous medium. Indeed, in the former case the silica content stabilizes around 35 wt%, similar to the value reported by Martens *et al.* (8) for a silicon-rich SAPO-5 prepared from Ludox and cyclohexylamine as template. It also corresponds to the silicon content at the surface of crystallites of high-silicon SAPO-5 obtained by Young and Davis (9). In both cases, the molar fraction of silica in the gel was in the range 0.4–0.5, whereas in our case the highest molar fraction of silica is 0.33. Then, it can be concluded that, in our case, the addition of CTA to a two-liquid phase system promotes the incorporation of silicon into the AFI framework.

Figure 2 shows some SEM micrographs of samples B2 and B3, prepared in CTA system, and two samples obtained in aqueous solution from diluted ($w_g = 100$, A2) and concentrated ($w_g = 40$, A3) gels. The CTA samples consist of shape rounded aggregates of small crystallites. The average size of the aggregates is around 12 μm, Figs. 2a and 2c, but it is very difficult to determine the crystallite size due mainly to the absence of a well-defined morphology. However, it can be estimated to be well below ~0.5 μm, Figs. 2b and 2d.

The two samples synthesized from aqueous media also consist mainly in aggregates, although some differences in crystal size and morphology can be observed in the SEM micrographs (Figs. 2e–2h). Big elongated aggregates of ~16 μm composed of very tinny irregular particles are obtained in the diluted system (Fig. 2f), and barrel shape particles of ~8 μm are obtained for $H_2O/SiO_2 = 40$. In this last case, besides the common featureless crystallites building up the aggregates, some well-faceted hexagonal crystals, smaller than the aggregates, can also be distinguished (Figs. 2g and 2h).

Infrared Spectroscopy

Figures 3 and 4 show the IR spectra obtained in the adsorption–desorption process of pyridine for the low frequency region and the spectra of the calcined sample in the high frequency region, characteristic of hydroxyl group stretching vibration.

Figure 3 corresponds to the infrared spectra of the samples obtained in the aqueous medium with different water contents ($w_g = 40$ and 100) at a crystallization time of 48 h and a crystallization temperature of 443 K (A2 and A4) or 468 K (A3). Hydroxyl groups at 3745 and 3675 cm^{-1}, assigned respectively to terminal Si–OH and P–OH groups, and 3625 (high frequency) and 3524 cm^{-1} (low frequency) bridged hydroxyl groups are detected (8). The main difference among the samples prepared in aqueous medium consists in the Brönsted acid strength of the bridged hydroxyls. The sample prepared from dilute gel (A2) still retains a small fraction of pyridine after evacuation at 623 K, whereas no pyridinium ion is detected at that temperature in the sample obtained from a more concentrated gel (A4). Therefore, a small concentration of Brönsted sites of medium-strong acid character are present in the former sample.

Figure 4 presents the IR spectra obtained for the samples synthesized in the two-liquid phase medium in the presence of surfactant at a crystallization temperature of 443 K and crystallization time of 48 h. Weak bands of terminal silanol groups at 3745 cm^{-1} are observed in the samples with the lowest Si content (B1 and B2), whereas this band is very intense for the high silicon content sample (B4). This could be attributed to the presence of some residual amorphous silica blended with the SAPO-5 crystals in this sample, which could partially account for the high silica content of the solid. The Brönsted acid sites present in the sample with the lowest Si content (B1) does not retain pyridine at a desorption temperature of 623 K. However, as the silicon content increases, a relatively high fraction of pyridine is retained at that temperature, which reaches a maximum for sample B2 (~10 wt% SiO_2) and then decreases for sample B4. This

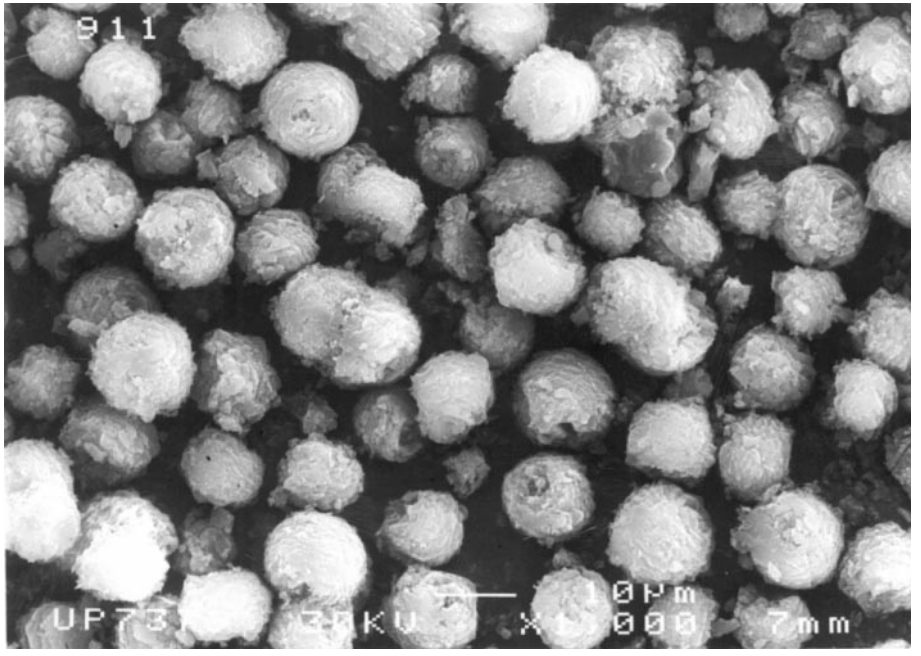
911
10µm
UP73 30KV X 000 7mm

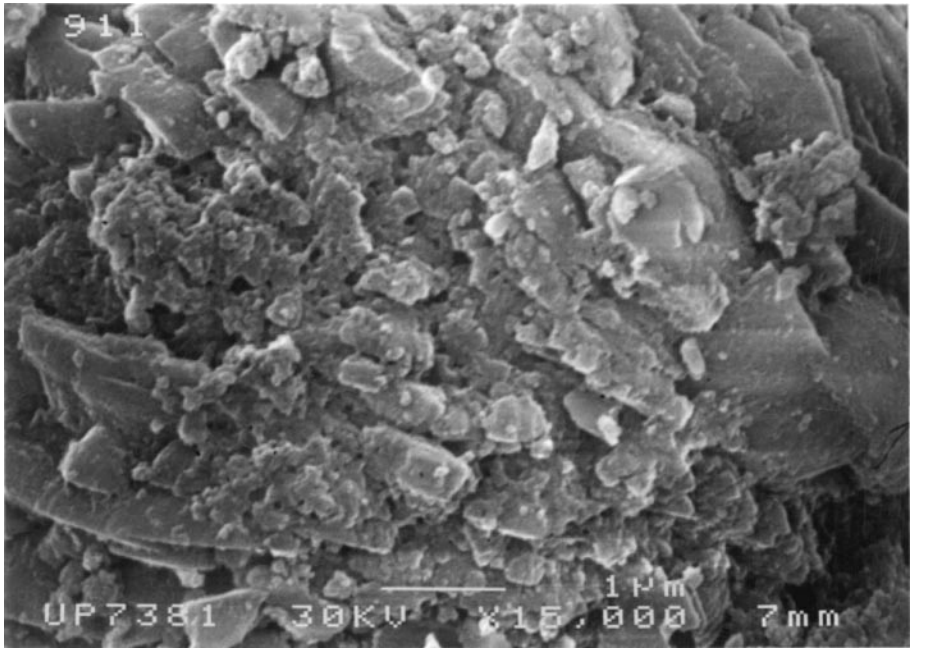
911
1µm
UP7381 30KV X15,000 7mm

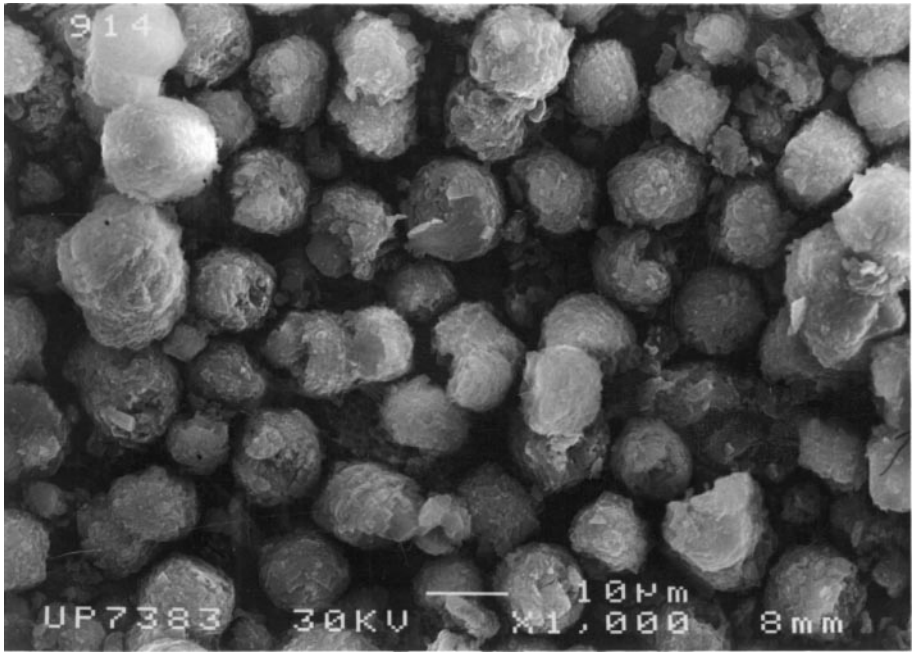
914
10µm
UP7383 30KV X1,000 8mm

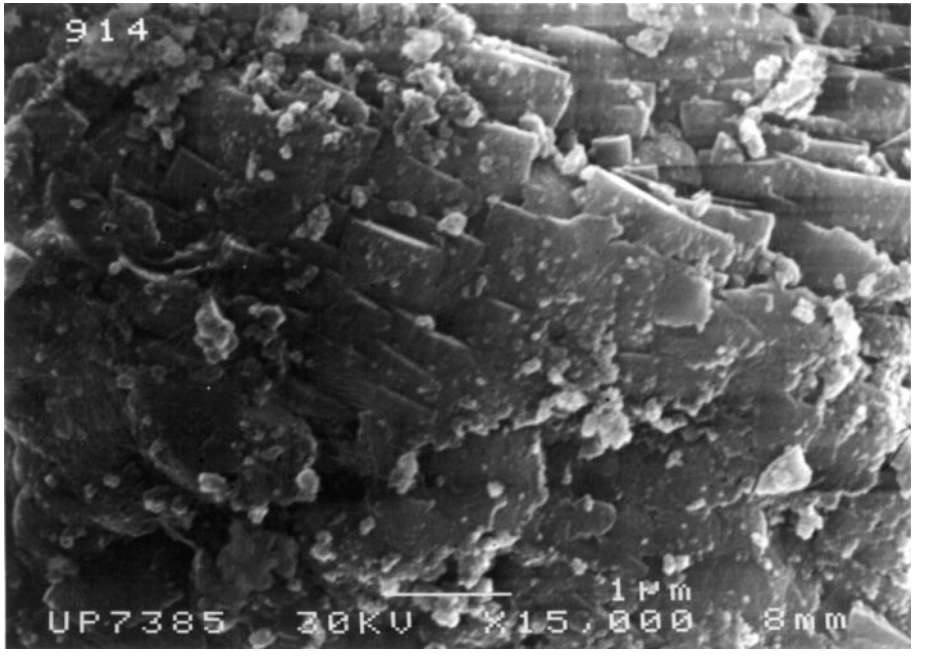
914
1µm
UP7385 30KV X15,000 8mm

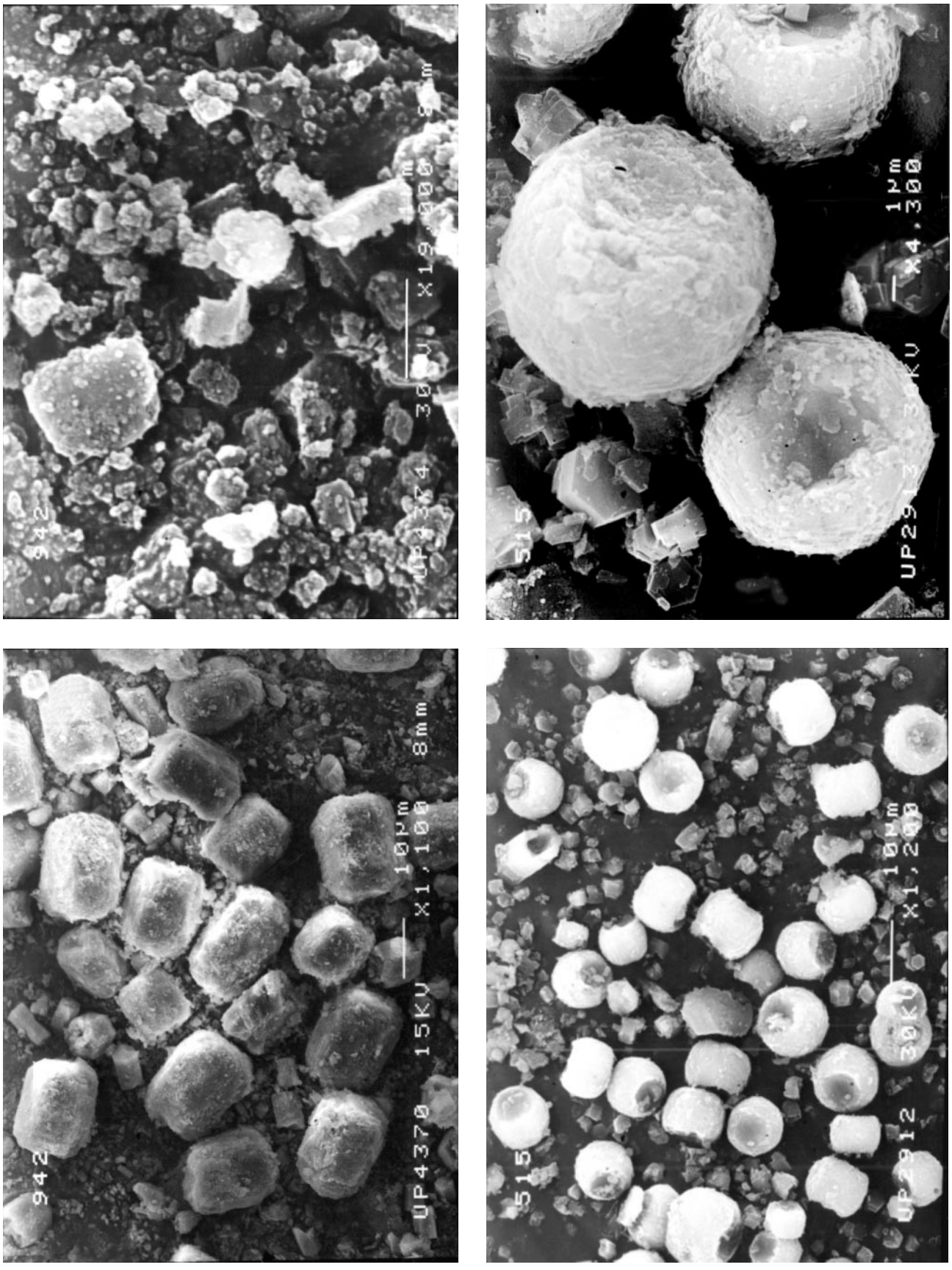

FIG. 2. SEM micrographs of samples B2 (a, b, top), B3 (c, d, bottom), A2 (e, f, top) and A3 (g, h, bottom).

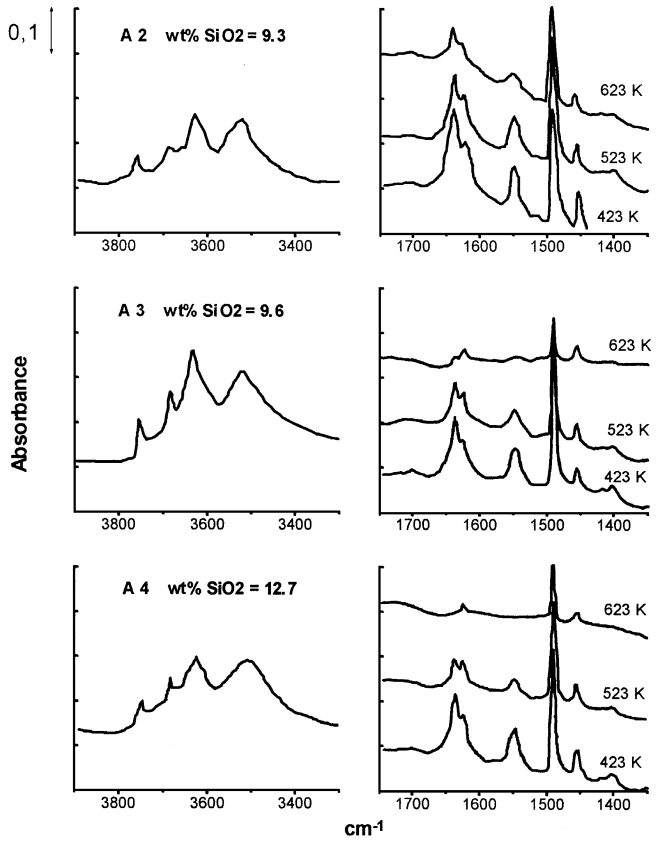

FIG. 3. IR spectra of SAPO-5 synthesized in aqueous medium.

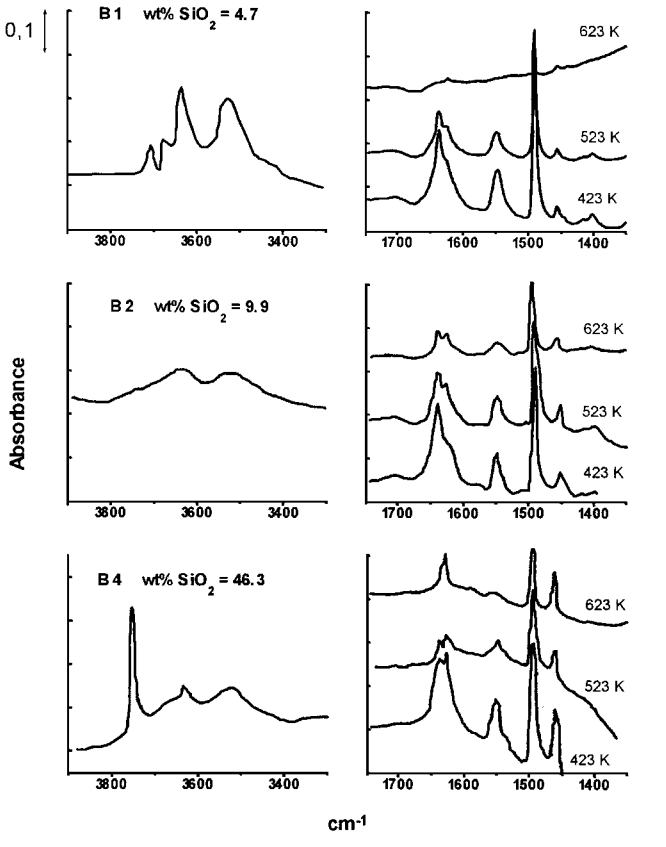

FIG. 4. IR spectra of SAPO-5 synthesized in two-liquid phase media.

indicates that the sample with intermediate Si content contains a higher amount of acid sites of medium-strong acid strength. Indeed, when the pyridine spectra of the samples having the strongest acidity prepared by the two methods are compared (A2 and B2), it can be seen that the fraction of medium-strong Brönsted acid sites is higher for the two-liquid phase sample.

Nuclear Magnetic Resonance Spectroscopy

Figure 5 shows the ^{27}Al MAS NMR spectra of some calcined samples prepared by the two methods (aqueous and two liquid phases). All spectra consist of an intense peak at 39 ppm typical of $Al(OP)_4$ tetrahedra in aluminophosphates, and two more signals of lower intensity at around 8 and −12 ppm, which are not unusual in calcined microporous $AlPO_4$ materials (10–12). The highest field resonance is characteristic of octahedral Al, usually assigned to framework aluminum atoms coordinated to two extra water molecules (10–12). The origin of the signal at 8 ppm is not so clear. In some cases it has been attributed to the presence of unreacted pseudobohemite (12). However, a more detailed ^{27}Al DOR NMR study in AlPO-5 led to the assignment of a relatively broad signal at ca 5 ppm to pentacoordinated Al due to the coordination of tetrahedral framework Al to one water molecule (11).

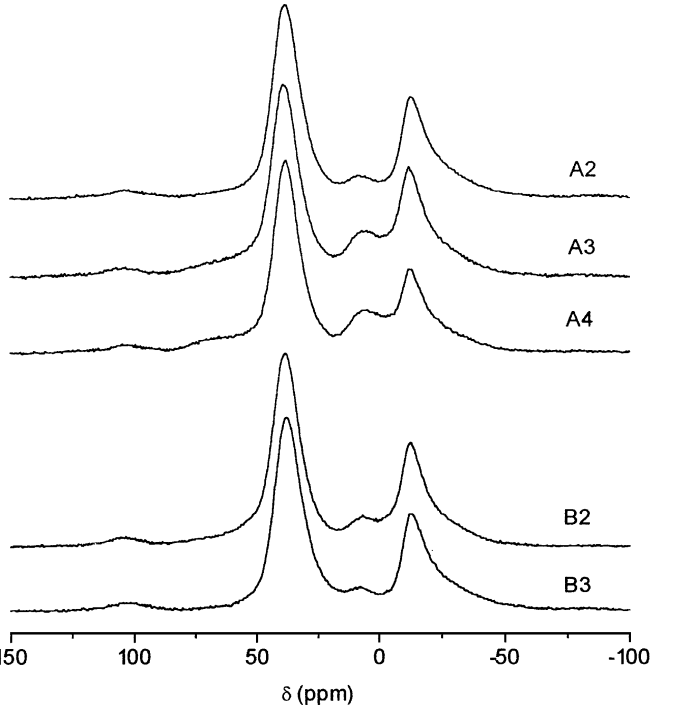

FIG. 5. ^{27}Al MAS NMR spectra of calcined samples.

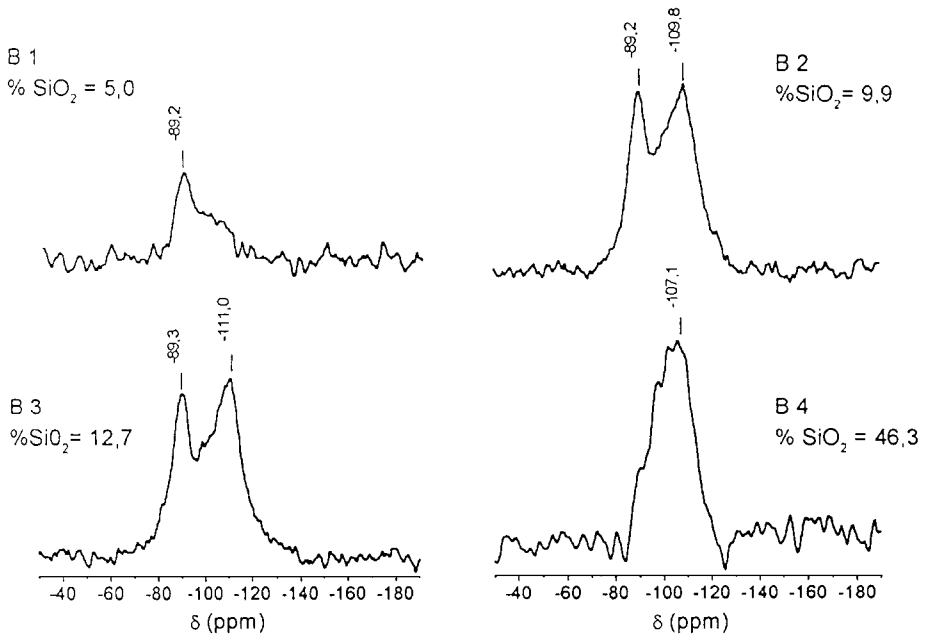

FIG. 6. ^{29}Si MAS-NMR spectra for SAPO-5 calcined samples obtained in the two-liquid phase medium.

^{29}Si MAS-NMR spectra of the samples synthesized in the two-liquid phase system, are shown in Fig. 6. For the sample with the lowest SiO_2 content (∼5%) the spectrum presents a predominant peak centered at −89 ppm, with some spectral features of lower intensity in the −100 to −110 ppm region. The main signal is attributed to Si(4Al), i.e., Si atoms with four Al atoms at the coordination shell (8). The appearance of this signal indicates substitution of P by Si via the SM2 model. By increasing the silicon content another signal appears at −110 ppm (B2 sample) which is attributed to Si(0Al), i.e. Si attached to four Si atoms in the coordination shell. For the Si richest sample (B4) the band at −110 ppm is the most intense in the spectrum and only smaller shoulders occur in the region situated between −90 to −110 ppm. The signal at −110 ppm is evidence of a combination of substitutions of a Si atom by a P atom and of two Si atoms by one P and one Al atom (SM2 + SM3) (8) and indicates the presence of silica islands in the crystals. We can conclude therefore that the mechanism of Si incorporation changes as a function of the Si content.

The ^{1}H → ^{29}Si CP/MAS-NMR spectra of samples with similar Si content (approximately 10%) synthesized in aqueous and two-liquid phase medium (Fig. 7) shows important differences between them.

The CP/MAS spectra of samples A2 and B2 are mainly formed by a peak at −90 ppm due to Si(4Al) and a broader signal with a maximum at ca −100 ppm. The chemical shift value of this latter component is typical of silanol groups. However, as the IR indicates that Si−OH groups are almost absent in sample B2 with a higher relative intensity of the component at −100 ppm, this resonance must be due to the presence of Si(nAl) species, $n = 1$–3, which occur mainly at the borders of the silicon domains (2, 13). Indeed, comparison of the ^{29}Si MAS NMR spectra of these two samples (A2 and B2) shows a high asymmetry at low fields of the signal at −110 ppm for sample B2 (see Fig. 8), indicating

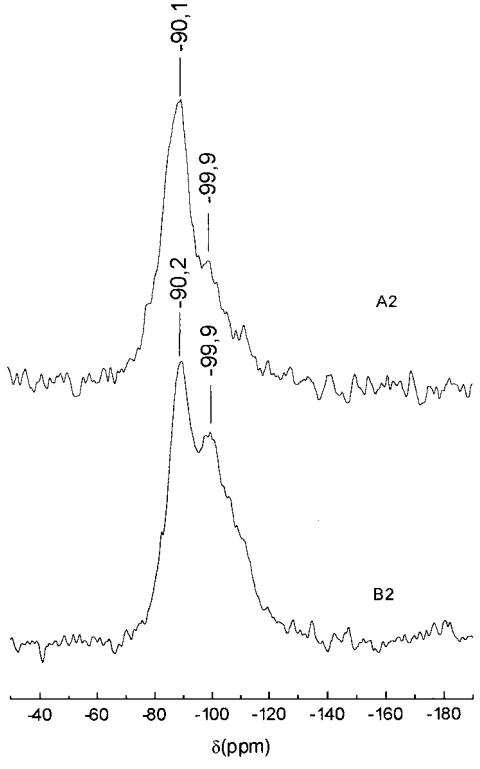

FIG. 7. ^{1}H → ^{29}Si CP/MAS NMR spectra for SAPO-5 calcined samples (a) aqueous medium, sample A2 (b) two-liquid phase medium, sample B2.

the contribution of other peaks in the −100 to −110 ppm region. Thus, we can suggest that the average size of the silicon domains should be smaller in the samples synthesized in the two-phase system than the corresponding samples obtained in the aqueous medium, increasing the total proton acid strength of the former sample.

In order to illustrate the different distribution of the Si environments in the samples obtained in the two-liquid phase and aqueous media, we have simulated the experimental ^{29}Si MAS NMR spectra of the samples with a Si content of ca 10 wt% (A2, A3, B2, and B3) as a sum of individual peaks as shown in Fig. 8. For the samples obtained in aqueous medium, the spectra can be simulated by only two signals at −90 and −110 ppm attributed to Si(4Al) and Si(4Si), respectively. On the contrary, two additional signals centered at −110 and −106 ppm are required to improve the spectra simulation of the samples obtained in the two-liquid phase medium, the first signal being more intense. The signal at −106 ppm can tentatively be attributed to Si(1Al) environment, whereas the signal at −100 ppm likely originates from contributions of Si(3Al) and Si(2Al) species. Then, Fig. 8 suggests a higher content of Si(nAl), $n = 1$–3 species in samples of series B.

It has been shown in an earlier paper (Ref. 4) that only cationic surfactants in the presence of n-hexanol and TEOS simultaneously are effective in reducing the average size of the Si islands. Moreover, only in these cases is CTA found in the SAPO-5 crystals. Although a detailed investigation of the synthesis mechanism is beyond the scope of this work, it can be speculated that in such a complex synthesis media the CTA would help in stabilizing silicate oligomers in the solution smaller than those present in pure aqueous solutions. Then, these small oligomers would be incorporated into the AFI framework during crystal growth.

It has been reported that relatively strong acid sites should be associated in SAPO-type materials with Si atoms with a first coordination shell partially populated by silicon (2). In the case of SAPO-37, it has been shown that the most active sites in acid-catalyzed reactions should be the ones located at the border of the Si islands (14). For this material, the formation of silicon patches by heating at 1000 K has been reported to increase the catalytic activity (15).

In our case, the CTA samples show higher acid strength by pyridine adsorption, in agreement with the NMR results. These changes in acidity due to changes in the Si environment should also influence the catalytic activity of the materials, and higher activity of the CTA samples should be expected. Indeed, this is the behaviour observed, as will be discussed below.

Catalytic Activity

The variation of the initial activity for *m*-xylene reaction as a function of the Si content of SAPO-5 synthesized in aqueous medium is shown in Fig. 9. As can be observed, for three sample series the initial activity increases up to a silica

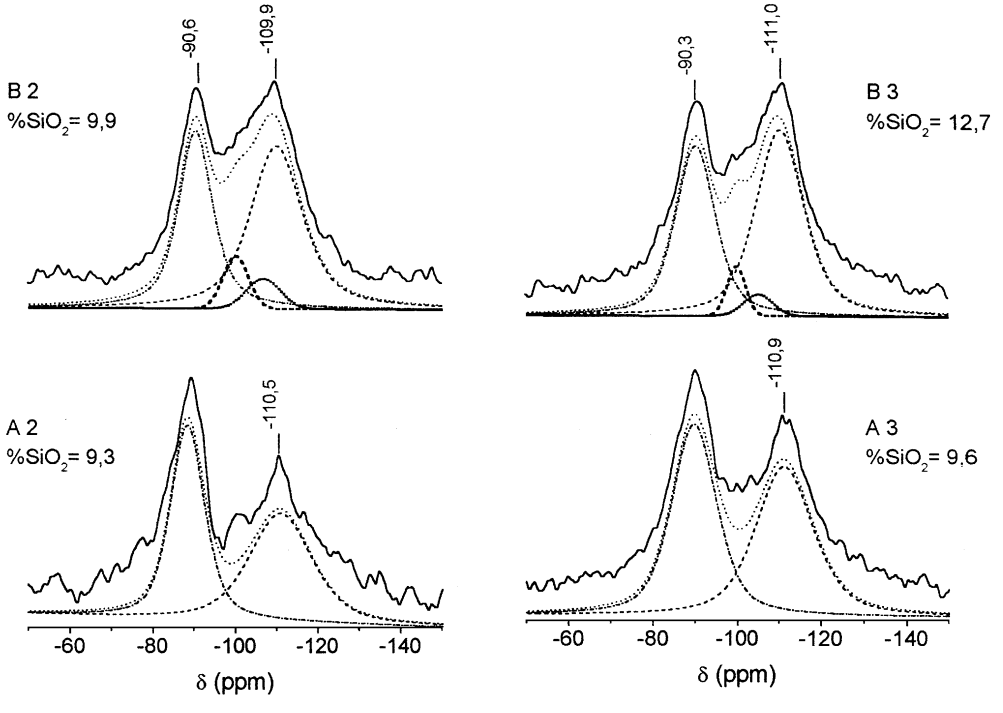

FIG. 8. ^{29}Si MAS-NMR spectra of SAPO-5 calcined samples synthesized in two-liquid phase medium (B2, B3) and aqueous medium (A3, A2). Experimental (———) and simulated (– – – – – –) spectra using the peak constituents (–· · –· · –· · –·, –·–·–·–·–, - - - - - - -, · · ·).

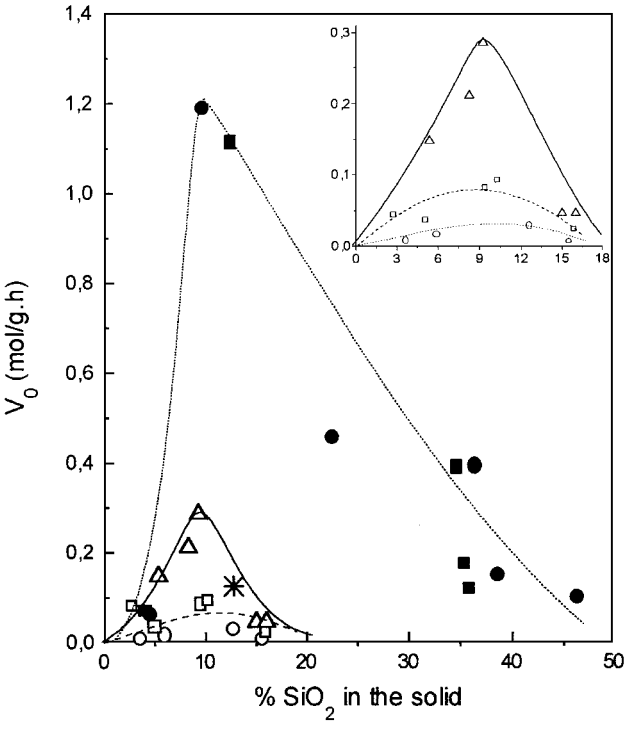

FIG. 9. Influence of silica content of SAPO-5 prepared in aqueous and two-phase medium on the rate of meta-xylene conversion. Symbols: same as in Fig. 1 and (Δ)$w_g = 100$ and 443 K; ($*$) two liquid phase synthesis without surfactant at 443 K.

content of about 10%, decreasing above this value. For the same Si content, the activity increases with crystallization temperature and with water content in the gel. It is worth mentioning that the maximum activity is obtained for the sample with the highest concentration of medium-strong acid sites, A2.

The sharp activity maximum displayed in Fig. 9 suggests that for very low Si content there would be a steady increase of acidity as the silicon incorporates into the crystals, but beyond the optimum Si value, a very rapid increase of the size of the silica islands occurs, which should strongly reduce both the total acidity and the average acid strength.

The activity pattern of the catalysts obtained in the hexanol/water/CTA system is also given in Fig. 9. It can be observed the same volcano-type variation of reaction rate as a function of the Si content described for the aqueous system, although the increase of activity is much sharper. This behaviour can be rationalized from the ^{29}Si MAS NMR and acidity results discussed previously. For small Si content, Si(4Al) acid sites of low acid strength are observed, which exhibits a low specific activity for *m*-xylene isomerization. For a silica content of ca 10 wt%, Si(4Al) environments coexist with small silica islands, where the hydroxyl groups associated to the Si atoms in the border between the Si domains and the SAPO-type structure have medium-strong acid strength. These acid groups would be the ones retaining pyridine after degassing at 623 K and they would be the ones responsible for the strong increase in reaction rate. The specific activity of these acid sites for *m*-xylene isomerization should be much higher than that of mild Si(4Al) sites, taking into account that the total acidity of the low Si content sample would be approximately the same as that of samples with maximum activity. As the Si content increases, both the total acidity and the number of the strongest acid sites would decrease, as a result of the preferential incorporation of silicon in large domains.

It can also be concluded that the strong enhancement of catalytic activity is due to the presence of CTA in the two-liquid phase system, since the sample synthesized in absence of surfactant from hexanol/water/TEOS system shows a much lower reaction rate.

However, the most remarkable aspect of the activity curves shown in Fig. 9 is the much higher reaction rates of the CTA samples. This enhancement of activity can hardly be accounted for by differences in crystal size. Indeed, in all the aqueous and CTA samples aggregates of submicron crystallites are observed, as was discussed above. Moreover, the para/ortho-xylene ratio (Table 2) is close to 1.0, indicating that these isomers are at the proportion determined by the chemical equilibrium and there is no shape-selectivity affecting the isomerization reaction, as expected for a large pore material with small crystal size. Then, the difference in activity between the two series of samples can also be explained by considering the model for Si substitution in AlPO-type framework discussed previously. The most active samples are those with the highest population of Si(nAl), $n = 1$–3, which are present at the border of the Si islands.

The I/D ratios (Table 2) of all the samples are characteristics of large pore monodirectional zeolites and molecular sieves catalysts (6). In our case, no striking differences

TABLE 2

Catalytic Results of Some Selected SAPO-5 Samples in the Reaction of *m*-Xylene

Sample	*m*-Xylene conversion (%)	Vo (mol/g · h)	P/O[a]	I/D[b]
A1	1.7	0.009	1.02	1.7
A2	4.5	0.285	0.97	3.8
A4	1.9	0.027	0.96	2.6
A3	4.7	0.083	0.87	3.4
B1	4.2	0.062	0.94	1.6
B2	6.1	1.190	1.10	4.3
B4	3.3	0.094	1.01	3.8
B3	7.3	1.110	1.l5	2.5

[a] P/O = para-xylene/ortho-xylene molar yields.

[b] I/D = (para-xylene + ortho-xylene)/ (toluene + $\sum$trimethylbenzenes) molar yields.

are observed between the aqueous and CTA samples, but nevertheless some variations in the I/D ratio are observed. This is not surprising, taking into account that the disproportionation reaction would be strongly affected, not only by the acid strength of the catalyst, but also by the acid site density in the framework (16–19). In regard to this, what the microscopic acid site distribution into the crystals might be is still unknown.

CONCLUSIONS

The effectiveness of Si incorporation into SAPO-5 depends on the synthesis method. More silicon is incorporated from two-liquid phase CTA containing gel. A maximum acid strength is obtained for CTA samples with SiO_2 content of ca 10 wt%. In the SAPO-5 synthesized in pure aqueous medium, the silicon is found mainly in Si(4Al) and Si(4Si) environments, while the samples synthesized in hexanol/water/CTA showed, besides these two Si coordination shells, also Si(nAl), $n = 1$–3, situated at the border of the Si islands. A strong increase in *m*-xylene isomerization is observed for the CTA containing system, which can be accounted for by the presence of medium-strong acid sites associated to these Si environments partially populated by aluminum.

ACKNOWLEDGMENTS

M. Montoya-Urbina acknowledge the Ministery of Education of Brazil and the Ministery for Foreign Affaires of Spain for a Ph.D. grant. Financial support by Comisión Interministerial de Ciencia y Tecnología (CICYT) of Spain (Project MAT 94-1035) is acknowledged.

REFERENCES

1. Wilson, S. T., Lok, B. M., Messina, C., Cannan, T. R., and Flanigen, E. M., *J. Am. Chem. Soc.* **104**, 1146 (1982).
2. Barthomeuf, D., *Zeolites* **14**, 394 (1994).
3. Martens, J. A., Grobet, P. J., and Jacobs, P. A., *J. Catal.* **126**, 299 (1990).
4. Franco, M. J., Mifsud, A., and Pérez-Pariente, J., *Zeolites* **15**, 117 (1995).
5. del Val, S., Blasco, T., Sastre, E., and Pérez-Pariente, J., *J. Chem. Soc. Chem. Comm.*, 731 (1995).
6. Martens, J. A., Pérez-Pariente, J., Sastre, E., Corma, A., and Jacobs, P. A., *Appl. Catal.* **45**, 85 (1988).
7. Treacy, M. M., Higgins, J. B., and von Ballmoos, R., *in* "Collection of Simulated XRD Powder Patterns for Zeolites," 3rd ed., Zeolites, Vol. 16, p. 323, (1996).
8. Martens, J. A., Mertens, M., Grobet, P. J., and Jacobs, P. A., *in* "Innovation in Zeolite Materials Science" (P. J. Grobet, W. J. Mortier, E. F. Vansant, and G. Schulz-Ekloff, Eds.), Stud. Surf. Sci. Catal., Vol. 37, p. 97, 1988.
9. Young, D., and Davis, M. E., *Zeolites* **11**, 438 (1991).
10. Kustanovich, Y., and Goldfarb, D., *J. Am. Chem. Soc.* **95**, 8818 (1991).
11. Jelinek, R., Chmelka, B. F., Wu, Y., Davis, M. E., Ulan, J. G., Gronsky, R., and Pines, A., *Catal. Lett.* **15**, 65 (1992).
12. Jahn, E., Müller, D., Wieker, W., and Richter-Mendau, J., *Zeolites* **9**, 177 (1989).
13. Man, P. P., Briend, M., Peltre, M. J., Lamy, A., Beaurnier, P., and Barthomeuf, D., *Zeolites* **12**, 563 (1991).
14. Martens, J. A., Jansens, C., Grobet, P., and Jacobs, P. A., *Stud. Surf. Sci. Catal.* **49**, 215 (1989).
15. Peltre, M. J., Man, P. P., Briend, M., Derewinski, M., and Barthomeuf, D., *Catal. Lett.* **16**, 123 (1992).
16. Ward, J. W., *J. Catal.* **17**, 355 (1970).
17. Karge, H. G., Ladebeck, J., Sarbak, Z., and Hatada, K., *Zeolites* **2**, 94 (1982).
18. Karge, H. G., Hatada, K., Zhang, Y., and Fiedorow, R., *Zeolites* **3**, 13 (1983).
19. Guisnet, M., *in* "Catalysis by Acid and Bases," Stud. Surf. Sci. Catal., Vol. 20, p. 283, (1985).